2500 m depth, or 10-30% of the speeds observed at the 500 m level. It is therefore easy to see why the Circumpolar Current has the largest mass transport of all ocean currents: It moves a slab of water more than 2000 meters thick with speeds comparable to other surface currents.

Another aspect which makes the Antarctic region unique is the unlimited communication with all other oceans. The fact that the hydrology of all ocean basins cannot be understood without insight into what goes on in Antarctic waters, provides us with the reason why we are looking at this region first.

Many oceanographers refer to the region around the continent of Antarctica as the *Southern Ocean*. The International Hydrographic Bureau, which is the authority responsible for the naming of oceanic features, does not recognize a sub-region of the world ocean of that name but includes its various parts in the other three oceans. Thus, the area between 146°55'E and 67°16'W (about 40%) is considered part of the Pacific Ocean, the area from 20°E to 146°55'E (about 35%) part of the Indian Ocean, and the area between 67°16'W and 20°E (the remaining 25%) part of the Atlantic Ocean. These definitions were developed and agreed upon before the central features of ocean dynamics discussed in the previous chapters were established. From an oceanographic point of view, subdivisions of the world ocean should reflect regional differences in its dynamics. The Southern Ocean certainly deserves its own name on that ground. While we took care not to use the term Southern Ocean for the chapter heading, we shall adopt it in this book from now on and define it as the region south of a line where the tropical/temperate dynamics of Figure 3.1 break down. This occurs where the permanent thermocline reaches the surface, i.e. in the Subtropical Convergence. Realistically, this is not a well defined line but a broad zone of transition, between tropical/temperate and polar ocean dynamics. Its southern limit is marked by a frontal region of limited width known as the Subtropical Front, which will be discussed in detail following the sections on the topography and on the wind regime. Within the limitations set by the time variability of the Subtropical Front, the surface area encompassed by the Southern Ocean represents roughly $77 \cdot 10^6$ km^2, or 22% of the surface of the world ocean.

Bottom topography

Since we expect the Circumpolar Current to be present at all depths we can anticipate that in the Southern Ocean the topography of the ocean floor has a much larger impact on the currents, and on the hydrology in general, than in any other ocean. Figure 6.2 shows that the Southern Ocean consists of three major basins, where the depth exceeds 4000 m, and three major ridges. The *Amundsen*, *Bellingshausen*, and *Mornington Abyssal Plains*, sometimes collectively called the Pacific-Antarctic Basin, extend eastward from the Ross Sea towards South America and belong fully to the Pacific sector of the Southern Ocean. They are separated from the basins of the temperate and tropical Pacific Ocean by the Pacific-Antarctic Ridge and the East Pacific Rise in the west and the Chile Rise in the east. The *Australian-Antarctic Basin,* which is located in the Indian Ocean sector, stretches westward from the longitude of Tasmania to the Kerguelen Plateau. The South-East Indian Ridge separates it from the Indian Ocean to the north, but communication with the basins of the eastern Indian Ocean below 4000 m depth is possible via a gap at 117°E. The *Enderby* and *Weddell Abyssal Plains*, also known as the Atlantic-Indian Basin, form part of the Atlantic and Indian Ocean sectors and reach westward from the Kerguelen Plateau to the

The *Kerguelen Plateau*, which carries a few isolated islands, reaches and nearly blocks the 2000 m level, although most of its broad plateau is between 2000 m and 3000 m deep. It leaves a narrow gap between itself and Antarctica through which flow can occur below the 3000 m level. No significant departure of the current direction across the plateau is observed.

Finally, south of eastern Australia and New Zealand the *Macquarie Ridge*, the *Pacific-Antarctic Ridge*, and the *South-East Indian Ridge* combine to form the third obstacle to the Circumpolar Current that reaches the 3000 m level. The only gap at that depth is located just south of the Macquarie Ridge, at 59°S. On the other hand, much of the Macquarie Ridge reaches above 2000 m, and the ridge carries three islands. The *Campbell Plateau*, a large expanse of water less than 1000 m deep, reaches 54°S just east of the ridge. As a result of the complicated topography and Coriolis force influence, the Circumpolar Current shows a clear northward deflection in this region.

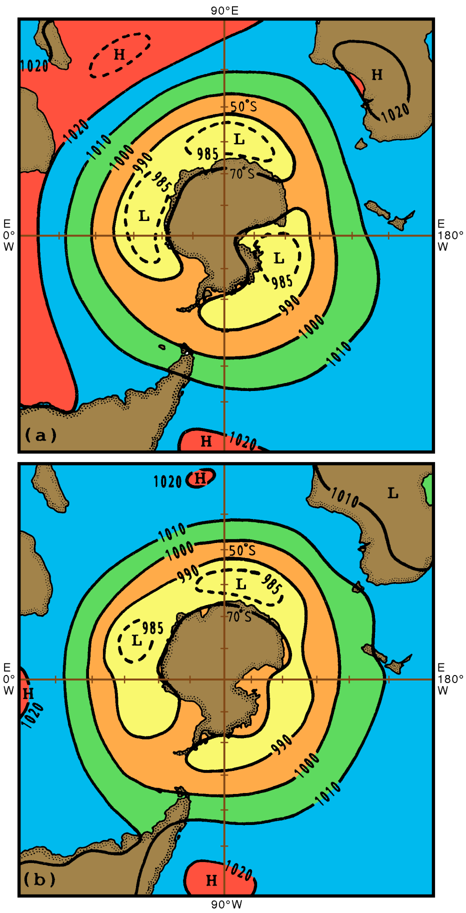

Fig. 6.3. (Left) Sea level air pressure (hPa) over the Southern Ocean. (a) July mean; (b) January mean. From Taljaard *et al.* (1969)

The wind regime

Most of the information required in this section is already included in Figures 1.2 - 1.4 and 4.3; but for the discussion of the Southern Ocean, projection on polar coordinates gives a better representation of the continuity around Antarctica. Figures 6.3 - 6.5 show the relevant maps. The surface pressure map (Figure 6.3) shows, in both summer and winter, a ridge of high pressure at about 25° - 35°S, with highest pressure over each ocean basin, and a trough at about 65°S, just north of the Antarctic continent. The mean geostrophic wind is evidently westerly between the trough and the ridge; but the mean pressure distribution strongly underestimates the mean wind stress which is proportional to the mean value of the square of the wind velocity. The circumpolar belt of westerly winds is dominated by frequent storms, which start in the north and angle southeastwards to die near 65°S where the winds turn into easterlies. It is these storms which determine the mean wind stress. The wind stress figures of Figure 6.4, which are based on the analysis of atmospheric observations over many years, include the transient

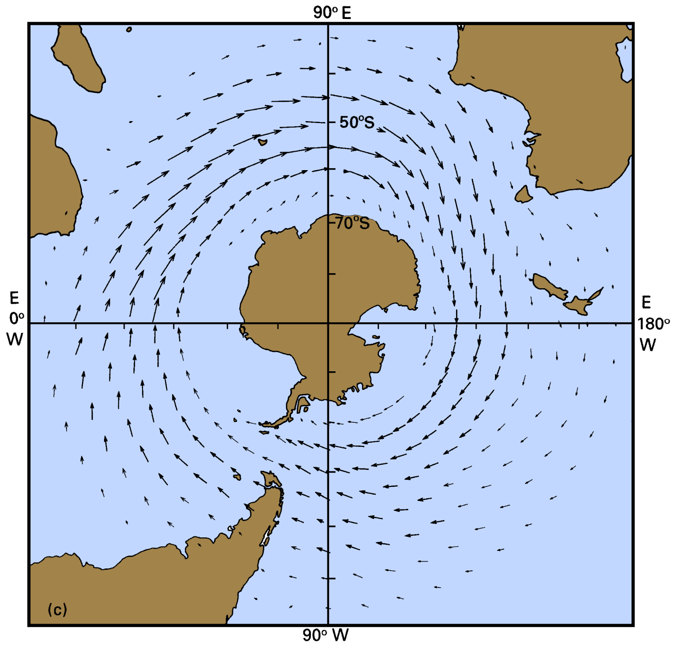

Fig. 6.4. (continued) Mean wind stress over the Southern Ocean (see Figure 1.4 for data sources).

(a, page 67) Annual mean;

(b, page 67) summer (December – February) mean;

(c, right) winter (June - August) mean.

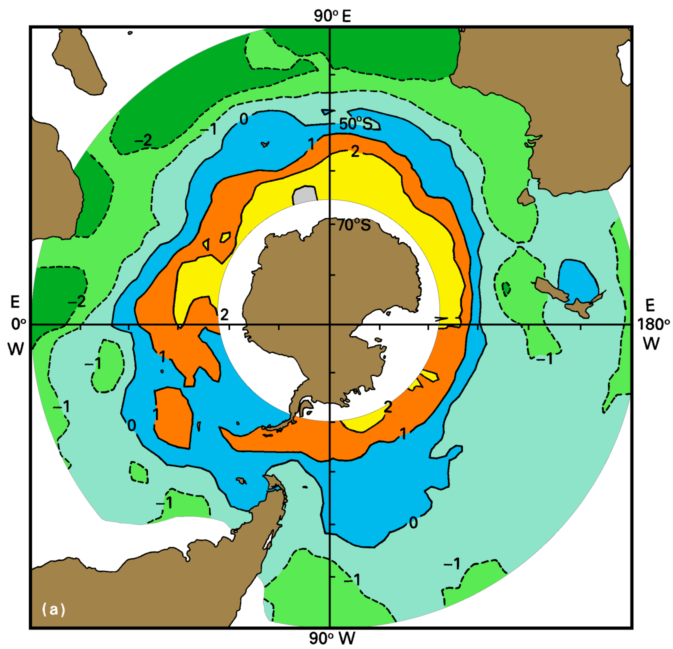

Close to the Antarctic continent the wind stress shows a reversal from eastward to westward, indicating the presence of Polar Easterlies along the coast. In the northern hemisphere the combination of West Wind Drift, Polar Easterlies, and meridional coastlines produces ocean currents known as the subpolar gyres (which will be discussed in later chapters). The Southern Ocean is devoid of meridional barriers, so the Polar Easterlies drive the *East Wind Drift*, a narrow coastal current which flows westward against the dominant eastward flowing Circumpolar Current. Both currents together are the southern hemisphere equivalent of the subpolar gyres.

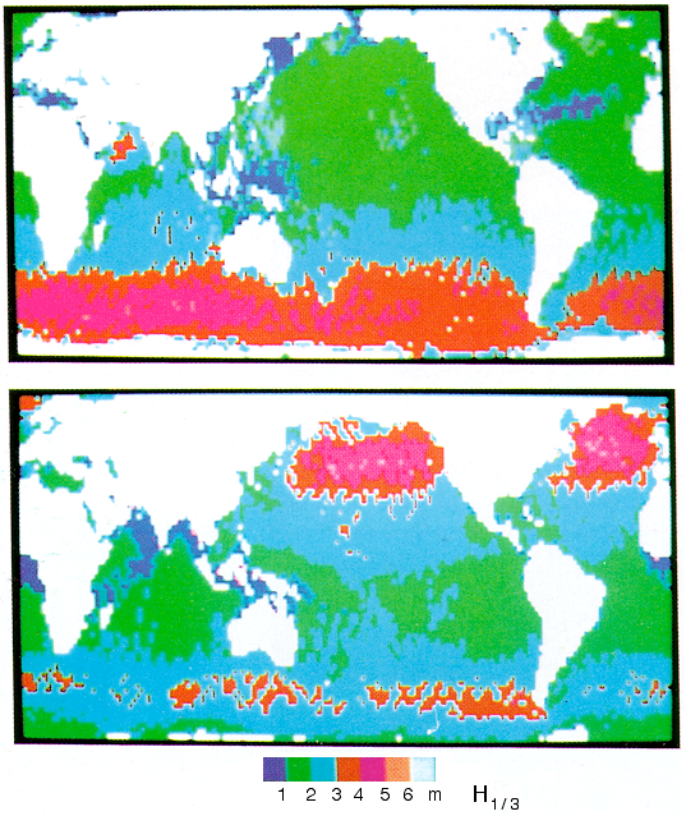

Fig. 6.6 Average significant wave height $H_{1/3}$ for the world ocean during the three-year period November 1986 – October 1989, determined from GEOSAT data. ($H_{1/3}$ is approximately the mean height of the 1/3 highest waves.) top: July, bottom: January. Note the prevalence of large waves ($H_{1/3}$ > 5m) in the Southern Ocean throughout the year, the increase in wave height during winter in both hemispheres, and the large waves in the western Arabian Sea during July. (See Chapter 11.)

One observation which stands out clearly in satellite data on the oceanic wave climate is the combined effect of consistently large wind speeds with little variation in wind direction, and no land barriers which could impede the build-up of a fully developed sea. The combination of infinite fetch around Antarctica and high average wind stress makes the Southern Ocean the region with the largest average wave height. Figure 6.6 shows results from GEOSAT, a satellite launched in March 1985 and active until October 1989. Wave data from GEOSAT were not available to non-military applications during the first eighteen months of its mission; the data used for Figure 6.6 are therefore restricted to a period between November 1986 and October 1989. This represents the best available estimate of annual mean conditions at present. The figure shows the Southern Ocean as a region of extremely high average wave height.

bounded by the two fronts (Figure 6.7). Close to the continent a separate water mass of uniform temperature and low salinity is found in the upper 500 m, separated from water of the Antarctic Zone by another frontal region, the continental water boundary.

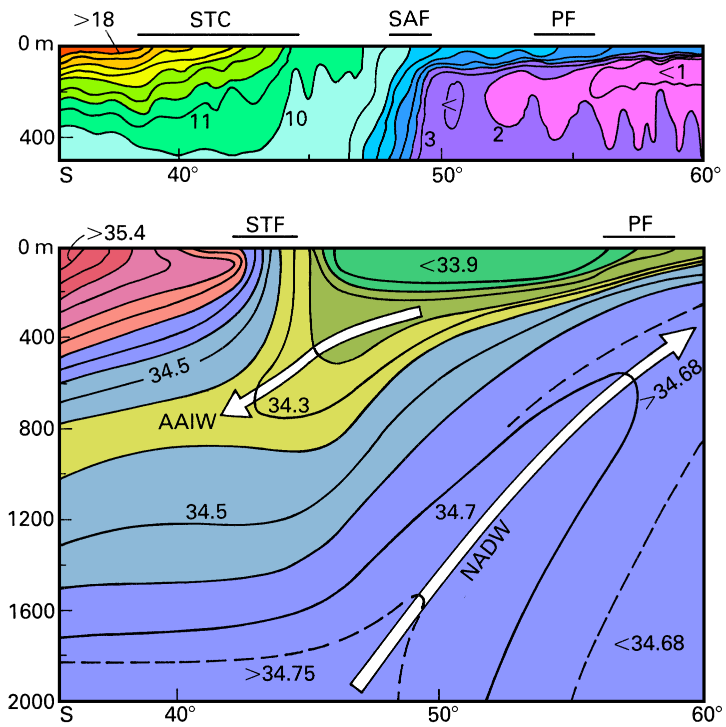

Fig 6.8. Hydrological sections through the Southern Ocean (summer conditions). (Top) Temperature section in the eastern Indian sector. The Polar Frontal Zone is indicated by the 3 - 9°C isotherms, and the split into the Subantarctic (SAF) and Polar (PF) Fronts by the crowding of isotherms at the surface around 7 - 9°C and 5 - 6°C. The Subtropical Front is indicated by the crowding of isotherms near 13 - 15°C within the Subtropical Convergence (STC). From Edwards and Emery (1982). (Bottom) Salinity section in the eastern Atlantic sector. Crowding of isohalines near 34.5 indicates the Subtropical Front. The Antarctic Divergence is located poleward of the section; near 65°S its salinity maximum is found just below 150 m. Upwelling of North Atlantic Deep Water (NADW) towards the divergence is indicated by the rise of the salinity maximum and sinking of Antarctic Intermediate Water (AAIW) from the Polar Front by the associated salinity minimum. Based on Bainbridge (1980). The different degree of detail between the two sections is the result of very different station density. See Fig. 6.2 for locations of sections.

In reality, the positions of the fronts and divergences vary greatly in time, and the intensity of sinking and rising motion is variable as well. There can be no doubt that the largest variability occurs in the Subtropical Front. Observations like those shown in Figure 6.9 usually indicate that the band of strong horizontal temperature and salinity

of averaging over a relatively narrow frontal region which changes its position over time. The Antarctic Polar Front and the Divergence appear to be less mobile than the Subtropical Front and therefore show up stronger in the long-term mean, but they, too, display high variability at least in time. This is seen in the paths of buoys tracked by satellite which in the region between the Polar Front and the Divergence typically show rapid movement for several hundred kilometers, followed by longer periods of quite slow movement.

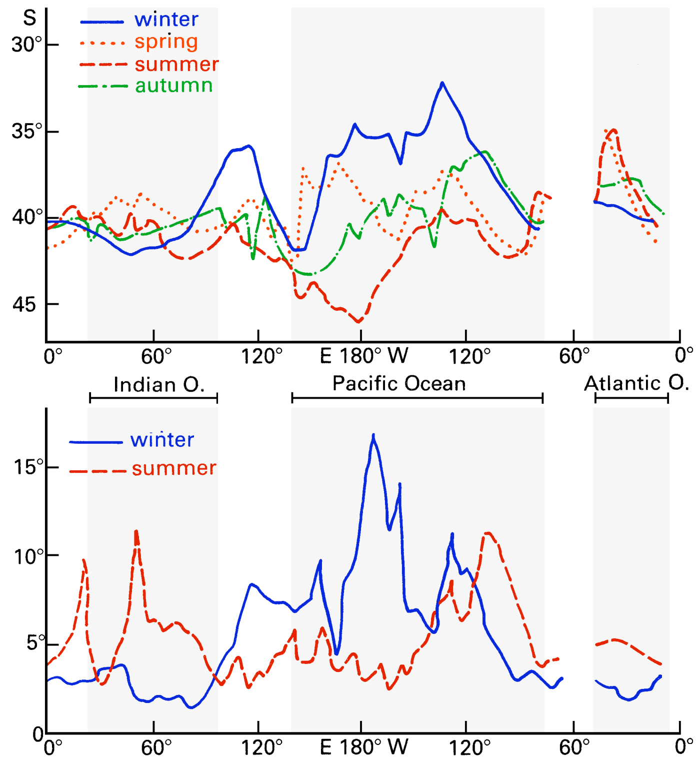

Fig. 6.10. (Right) Southernmost position of the 1015 hPa isobar during 1972-1977: (a) seasonal mean, (b) interannual variability, expressed as range (difference between largest northward and southward departure from the mean). Seasons are defined as: summer, December - March; autumn, April - May; winter, June - September; spring, October - November. Note the extreme seasonal and interannual variability in the Pacific Ocean. From Streten (1980).

The Antarctic Divergence, on the other hand, is linked with a meridional salinity maximum. At the surface the maximum is masked by low salinity from high precipitation and additional melting of ice, but it is clearly discernible below 150 m (Figure 6.8b). It is produced by upwelling of water with high salinity. The upwelling is unique in that the water reaching the surface comes from great depths; in the Atlantic Ocean, it is lifted from between 2500 m and 4000 m. The deep upwelling occurs for two reasons. Firstly, there is equatorward movement in the Intermediate Water and above, and again in the Bottom Water

the width and location of the various frontal zones. In the Indian Ocean sector, the Subantarctic and Subtropical Fronts merge near 95°E in the vicinity of the mid-ocean ridge (Edwards and Emery, 1982), and the Antarctic Polar Front merges with both above the Kerguelen Plateau near 65°E, eliminating the Subantarctic Zone completely (Gamberoni *et al.*, 1982).

Precipitation and ice

If collecting wind data in the Southern Ocean is difficult, collecting rain and snowfall data on the deck of a ship in gale force seas is positively unpleasant. It is therefore not surprising that our information on the mass exchange between the atmosphere and the ocean is particularly scarce in that region. A broad band of relatively high precipitation surrounds Antarctica, centered at about 50°S, the regions of the strongest winds. Since evaporation in these high latitudes is very low, the mass budget between ocean and atmosphere is dominated by fresh water gain for the ocean.

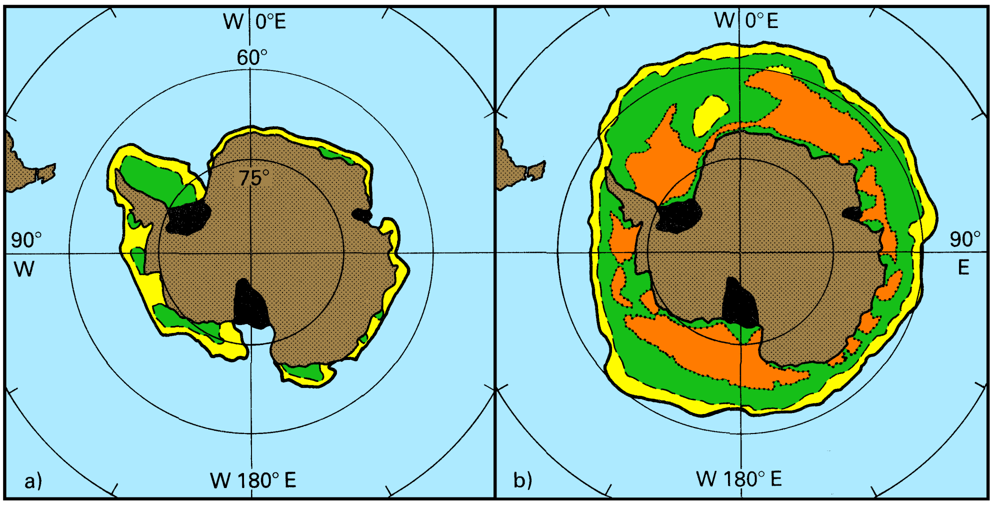

Fig. 6.12. Mean seasonal ice conditions in Antarctica, based on satellite data for 1973 - 1976. (a) Late summer (February), (b) late winter (October). Black areas indicate ice shelf (regions where the ice sits on the ocean floor): the ice shelves of the Weddell Sea at 50°W, the Ross Ice Shelf at the date line, and the Amery Ice Shelf at 70°E. The solid, broken, and dotted lines indicate ice coverage of 15%, 50%, and 85%.

The effect of precipitation on sea surface salinity is augmented by the loss of salt from the surface in winter, as brine rejected by sea ice sinks to great depth, and the melting of ice in summer; this explains the low salinity of near-surface water in the Antarctic region (Figure 2.5d). The sea ice does not extend far past Antarctica in summer, but it covers an area the size of the continent in late winter (Figure 6.12). Estimates of ice coverage from satellite data (Gloersen and Campbell, 1988) give the average ice extent for 1978-1987 as

Subantarctic Upper Water and 40% Circumpolar Water; only in the extreme eastern south Pacific Ocean and in the Scotia Sea of the Atlantic sector, where the T-S properties of Subantarctic Mode Water resemble those of Antarctic Intermediate Water, is Intermediate Water apparently formed in direct contact with the atmosphere. Formation of *Antarctic Circumpolar Water* through mixing of North Atlantic Deep Water and Antarctic Bottom Water is indicated by the straight line formed by T-S data between the Deep Water and the water on the Antarctic shelf.

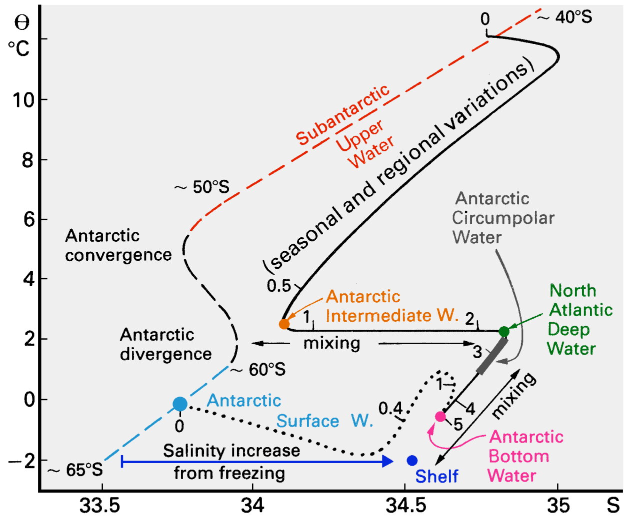

Fig. 6.13. A T-S diagram for a station in the Subantarctic (full line) and in the Antarctic zone (dotted line), and a T-S diagram from surface observations along crossings of the Antarctic Polar Front and Divergence (dashed line). Depth on the vertical T-S profiles is indicated in km.

It has of course to be remembered that the deep vertical and meridional circulation occurs on the background of intense zonal flow. This is particularly evident when the formation of Antarctic Bottom Water is investigated in detail. Its origin lies in deep convection at the continental shelf driven by the freezing of sea ice (Figure 6.13), but its final properties are shaped during intense mixing with the water of the Circumpolar Current (Circumpolar Water) while sinking to the bottom. It is therefore incorrect to say that the formation process for Antarctic Bottom Water is convection alone; rather, it is a combination of convection and subsurface mixing. It is seen that the properties of Circumpolar and Bottom Water are defined in a process of mutual interaction which draws on the properties of North Atlantic Deep Water as well.

The areas where convective sinking occurs (Figure 6.14a) are believed to be relatively limited in size. The only location where sinking to the ocean floor by convective overturning has been identified from data is Bransfield Strait; but the water which sinks there is collected in an isolated trough of between 1100 m and 2800 m depth and of little

with the Circumpolar Water. The properties of the sinking water are somewhat known from ships that have been trapped in the ice over winter. They measured bottom potential temperatures around the freezing point (about -1.9°C) and salinities of 34.7 -34.9. By the time the water leaves the Weddell Sea its temperature has risen to -0.8°C. The further path of Antarctic Bottom Water can be followed by looking at the potential bottom temperature map (Figure 6.15); it indicates the Adélie Shelf and the Ross Sea as other important regions where cold - and saline - water is injected from the surface. Eventually, the water spreads from the Circumpolar Current (i.e. with the properties of Circumpolar Water) into all three oceans. At that stage its properties are best described as 0.3°C and 34.7 salinity.

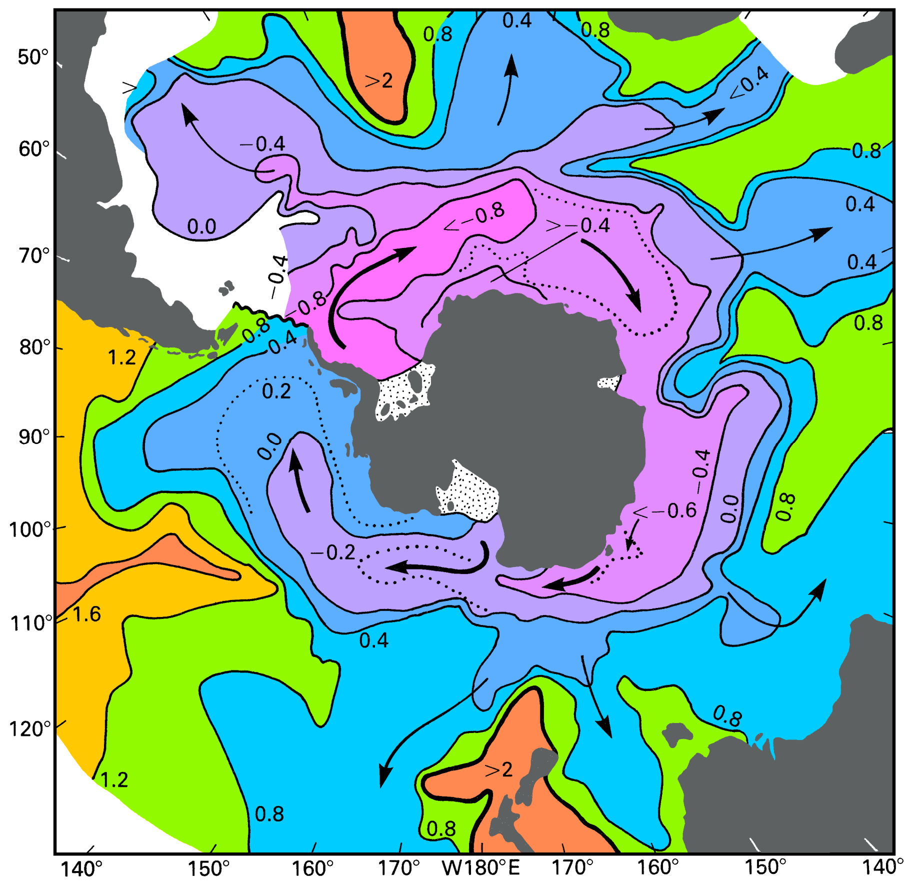

Fig. 6.15 Bottom potential temperature in the Southern Ocean. Isotherms are drawn every 0.4°C, with the exception of the New Zealand Plateau and the Mid-Atlantic Ridge where the 2°C isotherm follows the 0.8°C isotherm. The arrows show inferred movement of Antarctic Bottom Water. Southward intrusions of high potential temperatures reflect ridges less than 4000 m deep. Northward extensions of low potential temperatures indicate movement of Antarctic Bottom Water over sills; the deeper the sill, the lower the temperature. Adapted from Gordon (1986b).

of about four years, the mass transport for the Circumpolar Current through Drake Passage was determined as 128 ± 15 Sv, with maximum variations of over 50 Sv within two months and an indication of a winter minimum in July. Most of the mean transport could be accounted for by geostrophic flow above an assumed depth of no motion of 2500 m. The 50 Sv fluctuations were associated mostly with changes in sea level gradient across the passage with very little density change; the corresponding current variations were therefore uniform in depth. Earlier observations, for a one-year period and again in Drake Passage (Bryden and Pillsbury, 1977), gave an average of 139 Sv but a total range between 28 and 290 Sv. More definite estimates will become available with the completion of World Ocean Circulation Experiment (WOCE). Current speeds are generally low, between 0.05 and 0.15 m s^{-1}, because of the large width and depth of the current, although 0.5 m s^{-1} and even 1 m s^{-1} have been observed in jets associated with frontal regions on occasions. Because of their enhanced horizontal density gradients and associated geostrophic currents, the frontal regions carry most of the transport; observations from Drake Passage (Nowlin and Clifford, 1982) indicate that above 2500 m, 75% of the total flow occurs in the frontal zones, which occupy only 19% of the cross-sectional area.

Estimating the meridional heat flux, a key element in the global heat budget, is even more difficult. The transfer of heat from the Circumpolar Current to the atmosphere has been estimated (Gordon and Owens, 1987) as $3 \cdot 10^{14}$ W. This heat loss must be balanced against poleward oceanic heat flux across the current. The primary movers of heat appear to be the large eddies generated by the current in interaction with topography. Little is known about the frequency of eddy formation and the life expectancy of individual eddies. Satellite altimeter observations (Figure 4.8) imply that they are not uniformly distributed along the path of the Circumpolar Current but are more frequent east of the Scotia Ridge and in the region of the Macquarie Ridge (between Tasmania and New Zealand). These regions therefore are likely to play a major role in the poleward transport of heat. Temperature records from Drake Passage (Figure 6.17) indicate the passage of five cyclonic (i.e. cold core) eddies and one anticyclonic (warm core) eddy over a period of eight months. The eddies were of 30 - 130 km diameter, extended to at least 2500 m depth and were moving northward across the Circumpolar Current at about 0.04 m s^{-1}. This northward movement of (on average) cold water has to be compensated by poleward movement of comparatively warmer water and therefore represents a poleward flux of heat. Provisional estimates (Keffer and Holloway, 1988) give values of $1.3 - 5.4 \cdot 10^{14}$ W, enough to balance the estimated heat loss to the atmosphere.

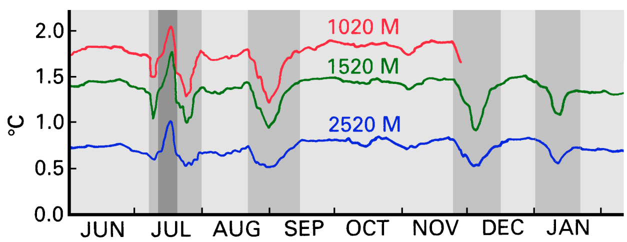

Fig. 6.17. A time series of temperature (°C) obtained at a mooring in central Drake Passage, showing the passage of five cold-core rings (medium shading) and one warm-core ring (dark shading). From Pillsbury and Bottero (1984).